Computer Coupling of Phase Diagrams and Thermochemistry 32 (2008) 432–438

Contents lists available at ScienceDirect

Computer Coupling of Phase Diagrams and Thermochemistry

journal homepage: www.elsevier.com/locate/calphad

Thermodynamic optimization of the Ga–Se system

F. Zheng [a], J.Y. Shen [b,*], Y.Q. Liu [c], W.K. Kim [d], M.Y. Chu [b], M. Ider [d], X.H. Bao [a], T.J. Anderson [d]

[a] Department of Chemistry, Shanghai University, Shanghai 200436, PR China
[b] General Research Institute for Nonferrous Metals, Beijing 100088, PR China
[c] School of Materials Science and Technology, China University of Geosciences, Beijing 100083, PR China
[d] Department of Chemical Engineering, University of Florida, Gainesville, FL 32611, USA

ARTICLE INFO

Article history:
Received 24 December 2007
Received in revised form
20 March 2008
Accepted 20 March 2008
Available online 21 April 2008

Keywords:
Ga–Se
Phase diagram
Thermodynamics
CALPHAD

ABSTRACT

As part of the construction of a Cu–In–Ga–Se quaternary thermodynamic database, which is essential to the optimization of a high-efficiency Cu(In, Ga)Se_2-based thin film solar cell process, a complete thermodynamic description for the Ga–Se binary system was established by thermodynamic optimization. The calculated thermodynamic properties and phase diagrams agree well with the experimental values.

1. Introduction

$CuInSe_2$-based thin film solar cells have attracted a lot of interest due to their excellent photovoltaic conversion efficiency (19.5% AM1.5G [1]), verified long-term outdoor stability, and the potential for lightweight and flexible cells. It is also found that the band gap engineering by the addition of gallium to $CuInSe_2$ (CIS) improves cell efficiency. The complex chemistry of the 4-component Cu(In, Ga)Se_2 (CIGS) system, however, makes the optimization of a high-efficiency CIGS synthesis process difficult. It is therefore necessary to understand the phase equilibrium and thermodynamic properties of the CIGS system, and ultimately establish a self-consistent thermodynamic database for the entire Cu–In–Ga–Se quaternary system. As part of this work, the sub-binary Ga–Se system has been thermodynamically optimized using related experimental data. Consequently, its complete thermodynamic description was established.

2. Review of the experimental data

2.1. Phase diagram

The phase diagram of the binary Ga–Se system has been investigated by several research groups [2–11] using differential thermal analysis (DTA), X-ray diffraction (XRD), microscopy and vapor pressure methods. It was reported that only two intermetallic compounds, i.e., GaSe and Ga_2Se_3, are stable in the Ga–Se system. Recent experiments demonstrate that GaSe, which shows a very limited homogeneity range, melts congruently at 1210–1211 K [5,6,9,10], which is relatively lower than earlier reported values, e.g., 1233 K [3,12] and 1223 K [4].

The Ga_2Se_3 has two polymorphs: a low-temperature stable β-Ga_2Se_3 in monoclinic structure and a high-temperature stable α-Ga_2Se_3 in cubic zinc-blende structure with a transition temperature of around 1000 K [7–9,13]. The α-Ga_2Se_3 phase shows a narrow composition range and melts congruently at around 1283 K [2,5,7–9]. A liquid immiscibility exists between Ga and GaSe with the monotectic temperature of about 1187 K. The liquid with a composition of ~55 at.% Se solidifies eutectically at around 1163 K to form GaSe and α-Ga_2Se_3 phases [6,7,9,10].

There were some discrepancies in the literature for the other features of the Ga–Se binary phase diagram. Rustamov et al. [3] suggested the existence of the Ga_2Se compound, which was excluded from the later equilibrium phase diagram [6,7,9] since this compound was found to be a mixture of Ga and GaSe. Ollitraut-Fichet et al. [7] reported the existence of the $GaSe_2$ compound and a miscibility gap at the Se-rich region (75–85 at.% Se) with a monotectic temperature of 1043 K, whereas other researchers [3,6,8,9,14] did not observe the $GaSe_2$ phase and the monotectic reaction in this region. Furthermore, Dieleman et al. [9] have claimed that there are other two metastable polymorphs of Ga_2Se_3, i.e., α'-Ga_2Se_3 and γ-Ga_2Se_3, which can be prepared by quenching a

* Corresponding author. Tel.: +86 10 82241314; fax: +86 10 64946980.
E-mail address: jianys@grinm.com (J.Y. Shen).

0364-5916/$ – see front matter © 2008 Elsevier Ltd. All rights reserved.
doi:10.1016/j.calphad.2008.03.004

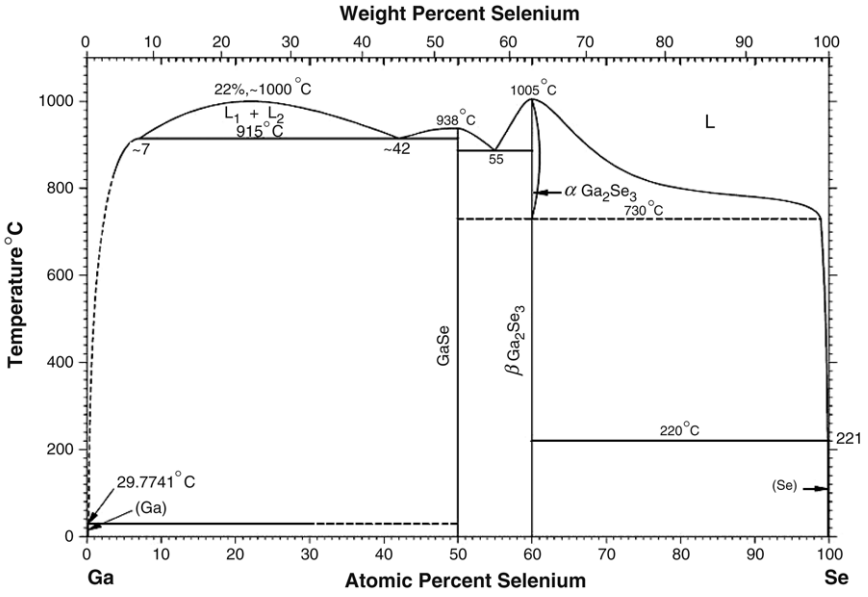

Fig. 1. Experimental Ga–Se binary phase diagram (taken from [15]).

melt and by heating the β-Ga_2Se_3 phase, respectively. As shown in Fig. 1, Massalski [15] summarized all experimental phase diagrams for the binary Ga–Se system over the entire composition range.

2.2. Thermodynamic properties

The thermodynamic properties for the intermediate compounds of the Ga–Se binary system have been extensively investigated as below:

GaSe: There are several reports in the literature [16–21] of the standard enthalpy of formation of GaSe at 298 K ($\Delta_f H^o_{298,GaSe}$). The values of $\Delta_f H^o_{298,GaSe}$, −146.44 ± 12.55 kJ/mol [16] and −158.992 ± 12.55 kJ/mol [18], were obtained from combustion calorimetry and galvanic cell data, respectively. Most recently, Zavrazhnov [21] has employed a new null-gage method measuring the equilibrium vapor pressure at different temperatures, created by the selective interaction of an ancillary component (e.g., GaI_3 and $GaCl_3$) with one of the components of a test sample (e.g., GaSe and Ga_2Se_3), to yield $\Delta_f H^o_{298,GaSe} = -157.7 \pm 0.9$ kJ/mol and the standard entropy at 298 K, $S^o_{298,GaSe} = 67.9 \pm 0.3$ J/mol K.

The heat capacity of GaSe has been investigated by [22–27]. Mamedov et al. [22] measured the heat capacities of GaSe using adiabatic calorimetry over the temperature range of 60.62 to 299.91 K, and derived the value of $S^o_{298,GaSe} = 70.29 \pm 0.7$ J/mol K. A few years later, they repeated the measurement of the heat capacities of GaSe covering a lower temperature range (i.e., 12–300 K), and reported the value of $S^o_{298,GaSe} = 70.25 \pm 0.2$ J/mol K [23]. Based on the multivariate regression of temperature dependence of heat capacity, Rymkevich et al. [24] obtained the values of $C_{P_{298,GaSe}} = 47.2$ J/mol K and $S^o_{298,GaSe} = 70.23$ J/mol K. The heat capacities of GaSe for a higher temperature region (50–600 K) were measured by Okhotin et al. [25]. Zavrazhnov et al. [26] extracted the temperature dependence of heat capacity for $Ga_1Se_{0.988}$, $Cp = 44.79 + 12.1 \times 10^{-3} \cdot T$ J/mol K(213 K < T < 543 K), from differential scanning calorimetry (DSC) measurement. Most recently, Tyurin et al. [27] have studied the heat capacity of GaSe by adiabatic calorimetry over the temperature range of 14 to 322 K yielding $C^o_{P298,GaSe} = 47.67 \pm 0.09$ J/mol K and $S^o_{298,GaSe} = 70.17 \pm 0.10$ J/mol K, which are almost identical to the previously reported values.

Ga_2Se_3: Calorimetry has been widely used to measure the standard enthalpy of formation of Ga_2Se_3 ($\Delta_f H^o_{298,Ga_2Se_3}$), e.g., $\Delta_f H^o_{298,Ga_2Se_3} = -439.32 \pm 12.55$ kJ/mol [16], −460.24± 20.92 kJ/mol [28], −376.56± 20.92 kJ/mol [29] and −368.61± 12.97 kJ/mol [30]. Later, Mamedov [18] used the galvanic cell data to obtain the values of $\Delta_f H^o_{298,Ga_2Se_3} = -405.01 \pm 20.92$ kJ/mol and -408.777 ± 12.55 kJ/mol by the Second and Third Law evaluation, respectively. It is, however, noted that there is a considerable discrepancy between the reported values of $\Delta_f H^o_{298,Ga_2Se_3}$.

Gadzhiev et al. [28] reported the heat capacity of Ga_2Se_3 at 298.15 K, i.e., $C^o_{p298,Ga_2Se_3} = 117.57$ J/mol K. Recently, an expression of the heat capacity for $Ga_1Se_{1.5}$ was deduced as $C_p = 53.25 + 15.6 \times 10^{-3} \cdot T$ J/mol K for 213 K < T < 543 K based on DSC measurements [26]. Tyurin et al. [31] have investigated the heat capacity of Ga_2Se_3 by adiabatic calorimetry over the temperature range of 14 to 320 K yielding $C^o_{p298,Ga_2Se_3} = 120.8 \pm 0.2$ J/mol K and $S^o_{298,Ga_2Se_3} = 180.4 \pm 0.4$ J/mol K.

Our research group has performed electromotive force (EMF) measurements to investigate the selected thermochemical properties and phase diagram of the binary Ga–Se system [13]. The EMF data of Ga–Se compounds were obtained for the composition of 55 and 65 at.% Se. The enthalpy for the transformation of β-Ga_2Se_3 to α-Ga_2Se_3 was calculated to be 17.2 kJ/mol, and the two transformation temperatures of 993.6 K and 1004 K were obtained from the two different cells. The expressions of the standard Gibbs energy of formation for β-Ga_2Se_3 and α-Ga_2Se_3 were deduced as $\Delta_f G^o_{\alpha\text{-}Ga_2Se_3} = -442.65 + 0.11816 \cdot T$ kJ/mol and $\Delta_f G^o_{\beta\text{-}Ga_2Se_3} = -425.46 + 0.10086 \cdot T$ kJ/mol (800 K < T < 1000 K). The detailed procedures and results for the above EMF experiments can be found elsewhere [13].

Liquid: Dieleman et al. [9] have measured the heats of fusion for the GaSe (56 ± 3.5kJ/mol) and Ga_2Se_3 (84 ± 7 kJ/mol) compounds by DTA. Mikkelsen et al. [14] have used the dew point method to measure the total Se vapor pressures of binary $Ga_{1-x}Se_x$, (0.6 < x < 1.0) in the temperature range of 700–1050 °C, and constructed a *P*–*T* diagram for the total Se pressure at compositions of 62, 65, 66.7, 70, 75 and 80 at.% Se. The activities of Se (α^l_{Se}) along the Se-rich liquidus have been also calculated from the total Se vapor pressure data.

3. Thermodynamic models

3.1. Pure elements

The Gibbs energy of the pure Ga or Se referred to the enthalpy of its stable state at 298.15 K (H_i^{SER}) is described as a function of temperature using the following equation:

$$^0G_i^{\varphi}(T) = G_i^{\varphi}(T) - H_i^{SER} = a + b\cdot T + c\cdot T\cdot \ln T + d\cdot T^2 + e\cdot T^3 + f\cdot T^{-1}\ (\mathrm{J/mol}) \quad (1)$$

where T is the absolute temperature, a, b, c, d, e and f are the coefficients to be determined. The superscript φ indicates the crystal structure of the phase. The Gibbs energy expressions for pure Ga($^oG_{Ga}^{\varphi}(T)$) and Se($^oG_{Se}^{\varphi}(T)$) are taken from the SGTE compilation [32] and reference [33], respectively. The author of [33] has carefully assessed the unary Se and found that the modification of Se descriptions in SGTE is necessary.

3.2. Stoichiometric compound

According to the experimental observation, both GaSe and β-Ga_2Se_3 phases are treated as stoichiometric compounds and their Gibbs energies are expressed by the following equation which is similar to Eq. (1) for pure elements.

$$^0G_{Ga_mSe_n} - m\cdot H_{Ga}^{SER} - n\cdot H_{Se}^{SER} = a + b\cdot T + c\cdot T\cdot \ln T + d\cdot T^2 + e\cdot T^3 + f\cdot T^{-1}\ (\mathrm{J/mol}) \quad (2)$$

where a, b, c, d, e and f are the coefficients to be optimized. The coefficients, c, d, e and f are directly related to the coefficients in the heat capacity equation for each compound, while a and b are mainly related to the enthalpies and entropies.

3.3. Liquid

The liquid phase is described by a two-sublattice ionic solution model [34] which can be schematically represented as $(Ga^{+3})_p(Se^{-2}, V_a^{-q}, Se)_q$, since this model describes the short range ordering effectively and is more straightforward to be extended to higher order systems compared to the associated solution model. The Ga^{+3} state is considered as the only species in the cationic sublattice, whereas its oxidized state Ga^{+2} is excluded due to its negligible amount. In addition to Se^{-2} state, neutral selenium (Se) and hypothetically charged vacancy (V_a^{-q}) are introduced into the anion sublattice to maintain the charge neutrality by adjusting the values of p and q.

The Gibbs energy of the liquid phase is expressed as:

$$G^L = {}^{ref}G^L + {}^{id}G^L + {}^{xs}G^L \quad (3)$$

where $^{ref}G^L$, $^{id}G^L$ and $^{xs}G^L$ are described as:

$$^{ref}G^L = y'_{Ga^{+3}}\cdot y''_{Se^{-2}}\cdot {}^0G^L_{Ga^{+3}:Se^{-2}} + q\cdot y'_{Ga^{+3}}\cdot y''_{V_a^{-q}}\cdot {}^0G^L_{Ga^{+3}:V_a^{-q}} + q\cdot y''_{Se}\cdot {}^0G^L_{Se} \quad (4)$$

$$^{id}G^L = RT\cdot q(y''_{Se^{-2}}\cdot \ln y''_{Se^{-2}} + y''_{V_a^{-q}}\cdot \ln y''_{V_a^{-q}} + y''_{Se}\cdot \ln y''_{Se}) \quad (5)$$

$$^{xs}G^L = y''_{Se^{-2}}\cdot y''_{Va^{-q}}\cdot L^L_{Ga^{+3}:Se^{-2},V_a^{-q}} + y''_{Se^{-2}}\cdot y''_{Se}\cdot L^L_{Ga^{+3}:Se^{-2},Se}. \quad (6)$$

In Eqs. (4)–(6), y'_A and y''_A represent the site fractions of state A in the first and second sublattice, respectively. Each interaction parameter (L) can be expressed by the series expansion of site fraction and the temperature dependence as below:

$$L = \sum_{\nu=0}^{n} {}^{\nu}L(y_i - y_j)^{\nu} \quad (7)$$

$$^{\nu}L = {}^{\nu}L_A + {}^{\nu}L_B\cdot T. \quad (8)$$

3.4. Non-stoichiometric compound α-Ga_2Se_3

The non-stoichiometric α-Ga_2Se_3 compound has the cubic zinc-blende structure with the space group of $F\bar{4}3m$. In this structure, Ga and Se atoms occupy different sites, and the third site of metal remains unoccupied [35]. No information is, however, available concerning the structure of this compound when its composition deviates from stoichiometry. To simplify the model by excluding too many unknown parameters, the α-Ga_2Se_3 phase is, therefore, described by the two-sublattice model of $(Ga, V_a)_2(Se, V_a)_3$.

The Gibbs energies of α-Ga_2Se_3 are expressed by the following equations:

$$^{ref}G^{\alpha} = y'_{Ga}y''_{Se}\,{}^{\circ}G^{\alpha}_{Ga:Se} + y'_{Ga}y''_{Va}\,{}^{\circ}G^{\alpha}_{Ga:Va} + y'_{Va}y''_{Se}\,{}^{\circ}G^{\alpha}_{Va:Se} + y'_{Va}y''_{Va}\,{}^{\circ}G^{\alpha}_{Va:Va} \quad (9)$$

$$^{id}G^{\alpha} = RT[2(y'_{Ga}\ln y'_{Ga} + y'_{Va}\ln y'_{Va}) + 3(y''_{Se}\ln y''_{Se} + y''_{Va}\ln y''_{Va})] \quad (10)$$

$$^{xs}G^{\alpha} = y'_{Ga}y'_{Va}\left[y''_{Se}\left({}^0L^{\alpha}_{Ga,Va:Se} + {}^1L^{\alpha}_{Ga,Va:Se}(y'_{Ga} - y'_{Va})\right) + y''_{Va}\left({}^0L^{\alpha}_{Ga,Va:Va} + {}^1L^{\alpha}_{Ga,Va:Va}(y'_{Ga} - y'_{Va})\right)\right] + y''_{Se}y''_{Va}\left(y'_{Cu}\,{}^0L^{\alpha}_{Ga:Se,Va} + y'_{Va}\,{}^0L^{\alpha}_{Va:Se,Va}\right) \quad (11)$$

where the superscript α represents α-Ga_2Se_3 phase. In Eq. (9), $^{\circ}G^{\alpha}_{Ga:Se}$ is the standard Gibbs energy of the stoichiometric α-Ga_2Se_3, and $^{\circ}G^{\alpha}_{Ga:Va}$ and $^{\circ}G^{\alpha}_{Va:Se}$ are expressed as:

$$^{\circ}G^{\alpha}_{Ga:Va} = 2\,{}^{\circ}G^{ort}_{Ga} + a_1 + b_1\cdot T \quad (12)$$

$$^{\circ}G^{\alpha}_{Va:Se} = 3\,{}^{\circ}G^{tri}_{Se} + a_2 + b_2\cdot T \quad (13)$$

where $^{\circ}G^{ort}_{Ga}$ and $^{\circ}G^{tri}_{Se}$ are the standard Gibbs energies for pure Ga in orthorhombic structure and pure Se in trigonal structure, respectively, and a_i and b_i are the parameters to be evaluated.

4. Results and discussion

The optimization of thermodynamic parameters for the Ga–Se binary system was performed using the PARROT program in the Thermo-Calc software [36]. Phase diagram and properties diagrams were calculated using the POLY3 program incorporated in the Thermo-Calc software. The optimization procedure was as follows. First, the initial estimates for the Gibbs energy of the compounds GaSe and β-Ga_2Se_3 were deduced from the reported values for the enthalpy of formation, standard entropy and heat capacity. Secondly, the Gibbs energy of the α-Ga_2Se_3 was estimated from the β-Ga_2Se_3 to α-Ga_2Se_3 transition temperature and corresponding enthalpy of transition. Thirdly, a rough optimization of the liquid coefficients was carried out considering the miscibility gap, the activities of selenium and the three phase equilibria involving liquid phase. Finally, the entire model parameters for all phases were optimized on the basis of all available experimental data.

The thermodynamic model parameters determined from this work were summarized in Table 1. The calculated Ga–Se phase diagram was compared with experimental data in Fig. 2(a). Enlarged comparison was given in Fig. 2(b) for the composition range of 35 to 65 at.% Se. A good agreement was achieved throughout the phase diagram with the only exception of Se-rich liquidus due to the scattered experimental data.

The experimental and calculated values of the temperature and composition for all invariant reactions are summarized in Table 2. Most of the calculated invariant reaction temperatures and compositions are in good agreement with the experimental data. It should be pointed out that the congruent melting temperatures of the GaSe reported in [3,4,12] were not included in our optimization since their values are much higher than the recently reported ones [5–7,9,10]. The measured temperatures for the eutectic

Table 1
Thermodynamic model parameters of the Ga–Se system

Phase	T/K	Parameters
GaSe	10–150	${}^{\circ}G_{GaSe} = -167\,923.156 - 16.555 \cdot T + 6.47715 \cdot T \cdot \mathrm{Ln}(T) - 0.255535 \cdot T^2 + 0.00022 \cdot T^3 - 3.96626 \cdot T^{-1}$
	150–1210	${}^{\circ}G_{GaSe} = -172\,930 + 246.86952 \cdot T - 46.71833 \cdot T \cdot \mathrm{Ln}(T) - 0.005285 \cdot T^2 + 87978.84 \cdot T^{-1}$
β-Ga_2Se_3	10–150	${}^{\circ}G^{\beta}_{Ga_2Se_3} = -423\,618.3568 - 26.37 \cdot T + 11.7477 \cdot T \cdot \mathrm{Ln}(T) - 0.61834 \cdot T^2 + 0.000531667 \cdot T^3 + 391.21983 \cdot T^{-1}$
	150–1283	${}^{\circ}G^{\beta}_{Ga_2Se_3} = -433\,687.01371 + 564.05 \cdot T - 109.57 \cdot T \cdot \mathrm{Ln}(T) - 0.01565 \cdot T^2 + 138\,605.625 \cdot T^{-1}$
α-Ga_2Se_3	298–3000	${}^{0}G^{\alpha}_{Ga:Se} = {}^{\circ}G^{\beta}_{Ga_2Se_3} + 17\,190 - 17.758264 \cdot T$ ${}^{0}G^{\alpha}_{Ga:Va} = 2\,{}^{\circ}G^{ort}_{Ga} + 332\,398 + 230 \cdot T$ ${}^{0}G^{\alpha}_{Va:Se} = 3\,{}^{\circ}G^{tri}_{Se} + 129\,500$ ${}^{0}G^{\alpha}_{Va:Va} = 0$ ${}^{0}L^{\alpha}_{*:Se,Va} = -629\,518$ ${}^{0}L^{\alpha}_{Ga,Va:*} = -88\,127$ ${}^{1}L^{\alpha}_{Ga,Va:*} = -23\,907$
Liquid	298–3000	${}^{0}G^{L}_{Ga^{+3}:Se^{-2}} = {}^{o}G^{\beta}_{Ga_2Se_3} + 104\,510 - 82.824104 \cdot T$ ${}^{0}G^{L}_{Ga^{+3}:Va} = {}^{\circ}G^{liq}_{Ga}$ ${}^{0}L^{L}_{Ga^{+3}:Se^{-2},Se} = 54\,342.2395 - 18.755369 \cdot T$ ${}^{1}L^{L}_{Ga^{+3}:Se^{-2},Se} = -31\,547.4021 + 8.32255587 \cdot T$ ${}^{0}L^{L}_{Ga^{+3}:Se^{-2},Va^{-q}} = 427\,496.439 - 384.012113 \cdot T$ ${}^{1}L^{L}_{Ga^{+3}:Se^{-2},Va^{-q}} = 4656.70437 - 100.194451 \cdot T$ ${}^{2}L^{L}_{Ga^{+3}:Se^{-2},Va^{-q}} = -69\,084.2637$ ${}^{3}L^{L}_{Ga^{+3}:Se^{-2},Va^{-q}} = -19\,483.2614$
Ga	200–303	${}^{\circ}G^{ort}_{Ga} = -21\,312.331 + 585.263691 \cdot T - 108.2287832 \cdot T \cdot \mathrm{Ln}(T) + 0.227155636 \cdot T^2 - 0.000118575257 \cdot T^3 + 439954 \cdot T^{-1}$
	303–4000	${}^{\circ}G^{ort}_{Ga} = -7055.643 + 132.73019 \cdot T - 26.0692906 \cdot T \cdot \mathrm{Ln}(T) + 0.0001506 \cdot T^2 - 4.0173 \times 10^{-8} \cdot T^3 - 118332 \cdot T^{-1} + 164.547 \times 10^{21} \cdot T^{-9}$
Ga_liquid	200–303	${}^{\circ}G^{liq}_{Ga} = -15821.033 + 567.189696 \cdot T - 108.2287832 \cdot T \cdot \mathrm{Ln}(T) + 0.227155636 \cdot T^2 - 0.000118575257 \cdot T^3 - 7.017 \times 10^{-17} \cdot T^7 + 439954 \cdot T^{-1}$
	303–4000	${}^{\circ}G^{liq}_{Ga} = -1389.188 + 114.049043 \cdot T - 26.0692906 \cdot T \cdot \mathrm{Ln}(T) + 0.0001506 \cdot T^2 - 4.0173 \times 10^{-8} \cdot T^3 - 118332 \cdot T^{-1}$
Se	298–760	${}^{\circ}G^{tri}_{Se} = -6657.653 + 92.539695 \cdot T - 19.14 \cdot T \cdot \mathrm{Ln}(T) - 0.012295 \cdot T^2 + 2.6766666 \times 10^{-6} \cdot T^3$
	760–1500	${}^{\circ}G^{tri}_{Se} = -9059.16586 + 150.334216 \cdot T - 28.552 \cdot T \cdot \mathrm{Ln}(T)$
Se_liquid	298–918	${}^{\circ}G^{liq}_{Se} = -9809.19613 + 288.813417 \cdot T - 52.4 \cdot T \cdot \mathrm{Ln}(T) + 0.024925 \cdot T^2 - 5.455 \times 10^{-6} \cdot T^3$
	918–1150	${}^{\circ}G^{liq}_{Se} = +8433.1372 - 78.4769299 \cdot T + 5.399 \cdot T \cdot \mathrm{Ln}(T) - 0.035945 \cdot T^2 + 5.2016666 \times 10^{-6} \cdot T^3$
	1150–1500	${}^{\circ}G^{liq}_{Se} = -7460.61988 + 192.646347 \cdot T - 36 \cdot T \cdot \mathrm{Ln}(T)$

The unit of Gibbs energy is J/mol of atoms. The symbol * indicates Ga, Se or Va. The "tri" and "ort" are the abbreviations of trigonal and orthorhombic, respectively.

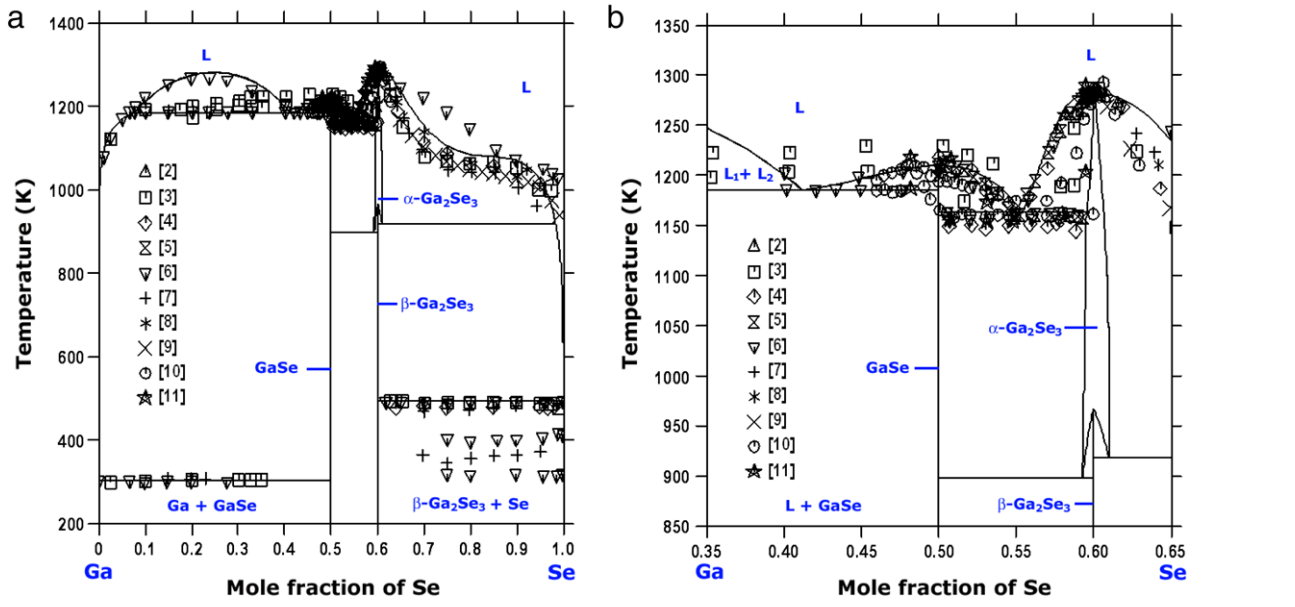

Fig. 2. Calculated Ga–Se binary phase diagram along with the experimental data. (a) The entire calculated phase diagram, (b) enlarged part of the calculated phase diagram ($0.35 < x_{Se} < 0.65$).

Table 2
The temperatures and compositions of the invariant reactions in the Ga–Se system

Reaction	Composition (at.% Se)	T (K)	Reaction type	Reference
$L \leftrightarrow L_1 + L_2$	~23	1268	Critical	[6]
	~24.3	1279		[7]
	~24	1267		[9]
	25.3	**1280**		**This work**
$L_1 + L_2 \leftrightarrow$GaSe	5.5/44/50	1188	Monotectic	[6]
	8.2/42/50	1187		[7]
	7.5/45.5/50	1190		[9]
	−/ − /~48	1185		[10]
	7.8/41.2/50	**1185**		**This work**
Ga + GaSe ↔ L	0/50/0	303	Eutectic	[3]
	0/50/0	303	(or peritectic)	[6]
	0/50/0	303		[7]
	0/50/0	303		[9]
	0/50/0	**303**		**This work**
GaSe ↔ L	50/50	1233	Congruent	[12]
	50/50	1233		[3]
	50/50	1223		[4]
	50/50	1211		[5]
	50/50	1211		[6]
	50/50	1218		[7]
	50/50	1210		[9]
	48.2/48.2	1210		[10]
	50/50	**1210**		**This work**
GaSe + α-Ga_2Se_3 ↔ L	50/60/55.0	1185	Eutectic	[3]
	50/59.76/55.4	1153	(or peritectic)	[4]
	50/59.4/55.1	1160		[5]
	50/60/55.0	1157		[6]
	50/60/55.0	1163		[7]
	50/60/55.1	1162		[9]
	−/ − /56.0	1161		[10]
	50/59.5/55.4	**1163**		**This work**
α-Ga_2Se_3 ↔ L	60/60	1293	Congruent	[12]
	60/60	1283		[2]
	60/60	1293		[3]
	60/60	1283		[4]
	60/60	1283		[5]
	60/60	1278		[6]
	60/60	1283		[7]
	60/60	1283		[8]
	60/60	1280		[9]
	60.6/60.6	1291		[10]
	60.04/59.9	**1283**		**This work**
GaSe + α-Ga_2Se_3 ↔ β-Ga_2Se_3	50/~59.9/~60.2	898	Eutectoid	[9]
	50/59.3/60	**898**		**This work**
β-Ga_2Se_3 ↔ α-Ga_2Se_3	60/60	1003	Polymorphic	[7]
	60/60	1003		[8]
	60.5/60.5	968		[9]
	60/60	994		[13]
	60/60	1004		[13]
	60/60	**967**		**This work**
β-Ga_2Se_3 + α-Ga_2Se_3 ↔ L	~60.7/61/−	918	Peritectic	[9]
	60/61/98.3	**918**		**This work**
β-Ga_2Se_3 + Se ↔ L	60/100/100	493	Eutectic	[3]
	60.24/100/100	478	(or peritectic)	[4]
	60/100/100	493		[6]
	60/100/100	493		[7]
	60/100/100	493		[9]
	60/100/100	**494**		**This work**

reaction GaSe + α-Ga_2Se_3 ↔ L lie in between 1185 K [3] and 1153 K [4], and our calculation (1163 K) is consistent with the recent experimental values [5–7,9,10].

The activities of Se (α^{l}_{Se}) along the Se-rich liquidus are displayed in Fig. 3. Moderate agreement was achieved between the calculated curves and the experimental values. The calculated heat capacities of the GaSe and β-Ga_2Se_3 are presented in Fig. 4(a) and (b), respectively. Despite a minor mismatch due to the scattered experimental data, the calculated heat capacities agree well with most of the measured data. The calculated entropies of the GaSe and β-Ga_2Se_3 were shown in Fig. 5(a) and (b), respectively, yielding the excellent fits to the experimental data.

The measured and calculated standard enthalpies of formation, standard entropies and heat capacities at 298.15 K for the

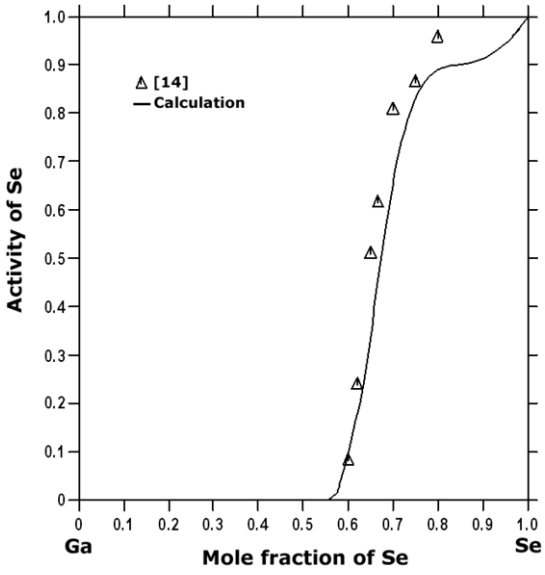

Fig. 3. Comparison between calculation and experiment for the activity of Se(α^{l}_{Se}) along the Se-rich liquidus. Reference state: Se(l).

intermetallic compounds GaSe and β-Ga_2Se_3 are summarized in Tables 3–5, respectively, where the calculated values are in excellent agreement with the measured ones, particularly the most recently reported ones [21,26,27,31].

The calculated enthalpy (17.19 kJ/mol) and temperature (967 K) for β-Ga_2Se_3 to α-Ga_2Se_3 transformation are almost identical to the experimental results of 17.2 kJ/mol [13] and 968 K [9]. It is worth noting that a considerable discrepancy exists among the measured temperatures of the polymorphic transition between β-Ga_2Se_3 and α-Ga_2Se_3. Even though the value reported in [9] is ~35 K lower than the others, the value in [9] has been adopted in this work. It is because the authors of [9] have measured various reactions related with the transitions among the polymorphisms of Ga_2Se_3, not only using several methods, but also considering the effect of oxygen to equilibrium.

Table 3
The standard enthalpies of formation ($\Delta_f H^{\circ}_{298}$) of the intermediate phases GaSe and β-Ga_2Se_3

Compound	$-\Delta_f H^{\circ}_{298}$ (kJ/mol)	Method	Reference
GaSe	146.44	Calorimetry	[16]
	143.5	Unknown	[17]
	158.992	Galvanic Cell	[18]
	158.992	Evaluation	[19]
	158.992	Evaluation	[20]
	157.7	Calorimetry	[21]
	157.941	**Evaluation**	**This work**
β-Ga_2Se_3	439.32	Calorimetry	[16]
	460.24	Calorimetry	[28]
	376.56	Calorimetry	[29]
	368.61	Calorimetry	[30]
	405.01/408.777	Galvanic Cell	[18]
	408.777	Evaluation	[19]
	408.777	Evaluation	[20]
	398.698	**Evaluation**	**This work**

Table 4
The standard entropy (S°_{298}) of the intermediate phases GaSe and β-Ga_2Se_3

Compound	S°_{298} (J/mol K)	Method	Reference
GaSe	70.29	Calorimetry	[22]
	68.9	EMF	[37]
	70.25	Calorimetry	[23]
	70.25	Calorimetry	[38]
	70.291	Evaluation	[19]
	70.23	Evaluation	[24]
	67.9	Calorimetry	[21]
	70.17	Calorimetry	[27]
	70.17	**Evaluation**	**This work**
β-Ga_2Se_3	183.26	Galvanic Cell	[18]
	179.912	Evaluation	[19]
	179.912	Evaluation	[20]
	180.4	Calorimetry	[31]
	180.7	**Evaluation**	**This work**

5. Conclusions

A self-consistent thermodynamic database for the Ga–Se binary system was obtained on the basis of available experimental data by the CALPHAD (CALculation of PHAse Diagram) method. Three intermetallic compound phases, GaSe, β-Ga_2Se_3 and α-Ga_2Se_3, were considered in the optimization, where GaSe and β-Ga_2Se_3 were treated as stoichiometric compounds and α-Ga_2Se_3 was

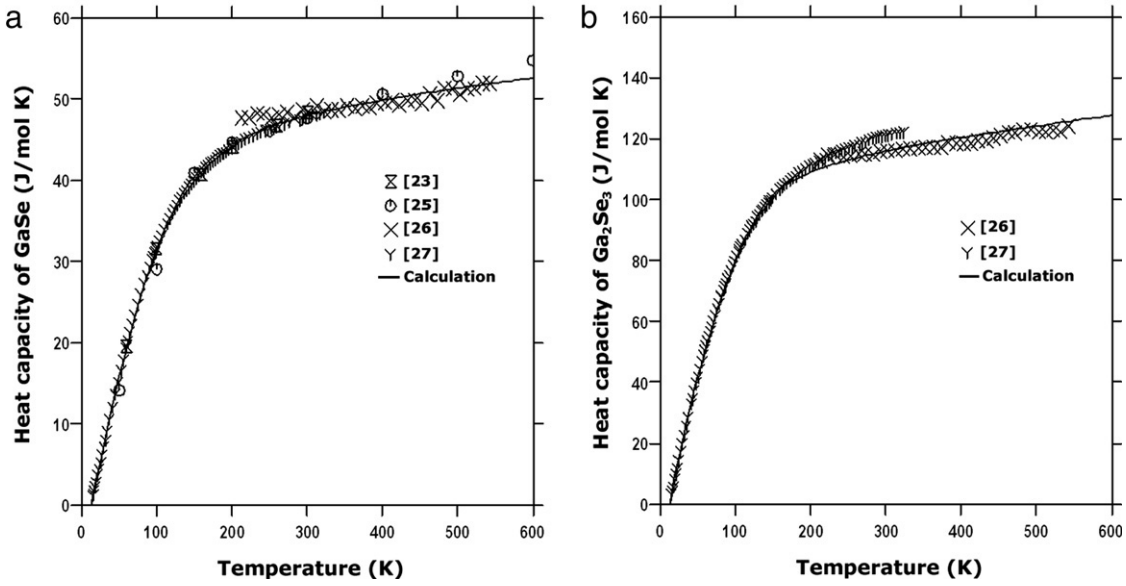

Fig. 4. Calculated heat capacities of GaSe and Ga_2Se_3 along with the experimental data.

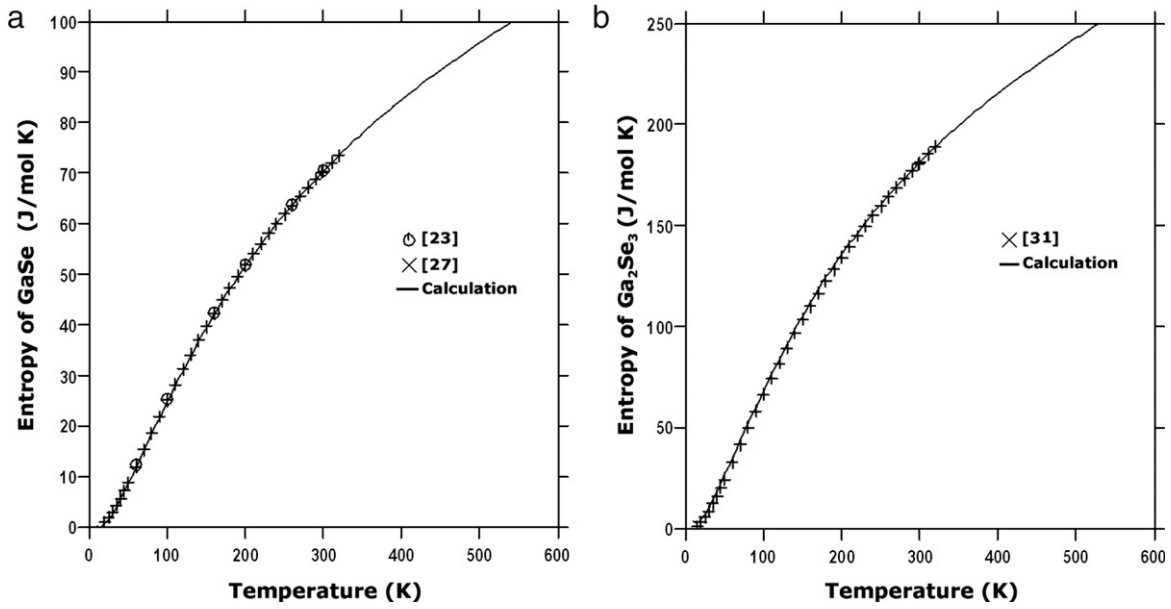

Fig. 5. Calculated entropies of GaSe and Ga_2Se_3 along with the experimental data.

Table 5
The heat capacity (Cp_{298}) of the intermediate phases, GaSe and β-Ga_2Se_3 at 298.15 K

Compound	Cp°_{298} (J/mol K)	Method	Reference
GaSe	48.49	Calorimetry	[22]
	48.51	Evaluation	[19]
	47.21	Evaluation	[24]
	47.79	Calorimetry	[25]
	47.67	Calorimetry	[27]
	48.32	Calorimetry	[26]
	47.89	**Evaluation**	**This work**
β-Ga_2Se_3	117.57	Calorimetry	[28]
	116.3	Evaluation	[19]
	115.8	Calorimetry	[26]
	120.8	Calorimetry	[31]
	115.8	**Evaluation**	**This work**

represented by a two-sublattice model. The liquid phase, which has shown immiscibility in the Ga-rich side, was described by the two-sublattice ionic liquid model. The calculated phase diagram and thermodynamic properties demonstrate a reasonable agreement with the measured data available in the literature.

Acknowledgements

Financial supports from the National Natural Science Foundation of China (NSFC) (Grant No.50672012) and the DOE/NREL Thin Film PV Partnership Program under subcontract No.ADJ-2-30630-13 are gratefully acknowledged. The authors would like to thank the Thermo-Calc Ltd. for providing the Thermo-Calc software.

References

[1] M.A. Contreras, K. Ramanathan, J. AbuShama, F. Hasoon, D.L. Young, B. Egaas, R. Noufi, Prog. Photovolt.: Res. Appl. 13 (2005) 209–216.
[2] L.S. Palatnik, E.K. Belova, Inorg. Mater. 1 (1965) 1703–1707.
[3] P.G.M. Rustamov, B.K. Babaeva, N.P. Luzhnaya, Inorg. Mater. 1 (1965) 775–776.
[4] L.S. Palatnik, E.K. Belova, Inorg. Mater. 2 (1966) 657–658.
[5] J. Dieleman, A.R.C. Engelfriet, J. Less-Common Met. 25 (1971) 231–233.
[6] H. Suzuki, R. Mori, Jpn. J. Appl. Phys. 13 (1974) 417–423.
[7] R. Ollitraut-Fichet, J. Rivet, ET J. Flahaut, J. Solid State Chem. 33 (1980) 49–61.
[8] J.C. Mikkelsen Jr., J. Solid State Chem. 40 (1981) 312–317.
[9] J. Dieleman, F.H.M. Sanders, J.H.J. Van Dommelen, Philips J. Res. 37 (1982) 204–229.
[10] V.I. Shtanov, A.A. Komov, M.E. Tamm, D.V. Atrashenko, V.P. Zlomanov, Dokl. Chem. 361 (1998) 140–143.
[11] A.Y. Zavrazhnov, D.N. Turchen, E.G. Goncharov, T.A. Prigorodova, Russ. J. Gen. Chem. 69 (1999) 1692–1697.
[12] W. Klemm, H.U. v. Vogel, Z. Anorg. Allge. Chem. 219 (1934) 45–64.
[13] I. Muhsin, Ph.D. Dissertation, University of Florida, Gainesville, FL, 2003.
[14] J.C. Mikkelsen Jr., G.B. Stringfellow, J. Phys. Chem. Solids 44 (1983) 1141–1145.
[15] T.B. Massalski, Binary alloy phase diagrams, Materials Park, Ohio: ASM International, 1990.
[16] H. Hahn, F. Burow, Angew. Chem. 68 (1956) 382.
[17] M.Kh. Karapetyants, M.L. Karapetyants, Principal Thermodynamic Constants of Inorganic and Organic Substances, Khimiya, 1968 (in Russian).
[18] K.K. Mamedov, Dissertat. for Examm. of Academic Degree for a Candidate in Tech. Sciences, Baku, Azerb., SSR., April 1969.
[19] K.C. Mills, Thermodynamic Data for Inorganic Sulphides, Selenides and Tellurides, Butterworth, London, 1974.
[20] I. Barin, G. Platzki, Thermochemical Data of Pure Substances, 3rd ed., Weinheim, 1995.
[21] A.Y. Zavrazhnov, Russ. J. Inorg. Chem. 48 (2003) 1577–1590.
[22] K.K. Mamedov, I.G. Kerimov, V.N. Kostryuko, H.M. Mekhtiev, Fiz. Tech. Poluprov. 1 (1967) 441–442.
[23] K.K. Mamedov, I.G. Kerimov, V.N. Kostryukov, M.I. Mekhtiev, Termodin. Termokhim. Konstanty (1970) 217–223.
[24] P.P. Rymkevich, P.G. Maslov, N.M. Zaitsev, Pao Hoang Van, Ban Vu Xuan, Zhur. Prikl. Khim. 48 (1975) 209–210.
[25] A.S. Okhotin, D. Uvdiev, G.L. Pervak, Deposited Doc., VINITI N1312-V98, 1998, pp. 10.
[26] A.Y. Zavrazhnov, D.N. Turchen, Zh.V. Dobrokhotova, V.V. Volkov, E.V. Makhonina, V.S. Pervov, Inorg. Mater. 40 (2004) 107–114.
[27] A.V. Tyurin, K.S. Gavrichev, V.E. Gorbunov, L.N. Golushina, A.D. Izotov, V.P. Zlomanov, Russ. J. Phys. Chem. 78 (2004) 1539–1542.
[28] S.N. Gadzhiev, K.A. Sharifov, Voprosy Met. i Fiz. Poluprovod., Akad. Nauk SSSR (1961) 43–45.
[29] G. Effendiev, S.S. Karaev, Khal'kogenidy Mater., Semin. 1 (1965) 133–140.
[30] K.A. Sharifov, T.Kh. Azizov, Zhur. Fiz. Khim. 41 (1967) 1208–1209.
[31] A.V. Tyurin, K.S. Gavrichev, L.E. Golushina, V.E. Gorbunov, V.P. Zlomanov, Inorg. Mater. 41 (2005) 1139–1143.
[32] A.T. Dinsdale, CALPHAD 15 (1991) 317–425.
[33] C.H. Chang, Ph.D. Dissertation, University of Florida, Gainesville, FL, 1999.
[34] M. Hiller, B. Jansson, B. Sundman, J. Ågren, Met. Trans. A 16A (1985) 261.
[35] H. Hahn, W. Klingler, Z. Anorg. Chem. 259 (1949) 135–142.
[36] B. Sundman, B. Jansson, J.-O. Andersson, CALPHAD 9 (1985) 153–190.
[37] A.S. Abbasov, K.N. Mamedov, P.G. Rustamov, P.K. Babaeva, Khim. Svyaz Poluprov. (1969) 200–202.
[38] I.G. Kerimov, K.K. Mamedov, V.N. Kostryukov, M.I. Mekhtiev, Teplofiz. Svoistva Tverd. Tel, Mater. Vses. Teplofiz. Konf. Svoistvam Veshchestv Vys. Temp. 3rd, 1971, pp. 202–210.